Article

Development of an Iminocoumarin-Based Zinc Sensor Suitable for Ratiometric Fluorescence Imaging of Neuronal Zinc

Kensuke Komatsu, Yasuteru Urano, Hirotatsu Kojima, and Tetsuo Nagano

J. Am. Chem. Soc., **2007**, 129 (44), 13447-13454• DOI: 10.1021/ja072432g • Publication Date (Web): 10 October 2007

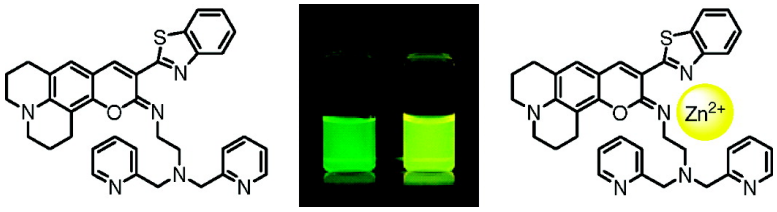

More About This Article

Additional resources and features associated with this article are available within the HTML version:

- Supporting Information
- Links to the 16 articles that cite this article, as of the time of this article download
- Access to high resolution figures
- Links to articles and content related to this article
- Copyright permission to reproduce figures and/or text from this article

View the Full Text HTML

J|A|C|S
ARTICLES
Published on Web 10/10/2007

Development of an Iminocoumarin-Based Zinc Sensor Suitable for Ratiometric Fluorescence Imaging of Neuronal Zinc

Kensuke Komatsu,[†,‡] Yasuteru Urano,[†,§] Hirotatsu Kojima,[†,‡] and Tetsuo Nagano*[,†,‡]

Contribution from the Graduate School of Pharmaceutical Sciences, The University of Tokyo, 7-3-1 Hongo, Bunkyo-ku, Tokyo 113-0033, and CREST and PRESTO, Japan Science and Technology Agency, 4-1-8 Honcho, Kawaguchi, Saitama 332-0012, Japan

Received April 6, 2007; E-mail: tlong@mol.f.u-tokyo.ac.jp

Abstract: Ratiometric imaging is a technique to reduce artifacts by minimizing the influence of extraneous factors on the fluorescence of a sensor and is particularly useful for cellular imaging studies. Here we characterized the iminocoumarin fluorophore as a new scaffold for sensors for ratiometric imaging. The iminocoumarin **4** showed a high quantum yield in aqueous media on excitation in the visible wavelength region, while its coumarin analogue showed little fluorescence. We therefore developed a novel fluorescence probe, ZnIC, for ratiometric imaging of Zn^{2+}, using iminocoumarin as a fluorophore and (ethylamino)-dipicolylamine as a Zn^{2+} chelator. ZnIC exhibited almost the same fluorescence properties as **4**, and the emission spectrum of this probe was red-shifted on addition of Zn^{2+} under physiological conditions. ZnIC is selective for Zn^{2+} over other biologically important metal ions, such as Ca^{2+} and Mg^{2+}, and has high affinity for Zn^{2+}. To confirm the suitability of ZnIC for biological applications, we employed it for the ratiometric detection of changes in intracellular Zn^{2+} in cultured cells and in rat hippocampal slices. The results indicate that iminocoumarin is a useful fluorophore for fluorescence microscopic imaging and that ZnIC should be useful for studies on the biological functions of Zn^{2+}.

Introduction

Fluorescence probes are excellent sensors for biomolecules and other biologically relevant targets, being sensitive, rapidly responsive, and capable of affording high spatial resolution via microscopic imaging.[1] They serve as useful tools for functional studies in biological systems.[2] Most currently available sensors signal the analyte concentration by an increase or decrease of the emission intensity. However, the emission intensity is also dependent on other factors, such as the sensor concentration, bleaching, optical path length, and illumination intensity. It is therefore desirable to eliminate the effects of these factors by using a ratiometric sensor that exhibits a spectral shift upon reaction or binding to the analyte of interest, so that the ratio between the two emission intensities can be used to evaluate the analyte concentration.[3]

This approach was originally developed for the visualization of calcium ion (Ca^{2+}) flux in living cells,[4] and a number of Ca^{2+} probes for ratiometric imaging are now commercially available, such as fura-2 and indo-1.[5] The many advantages of ratiometric measurement, combined with instrumental advances, make these sensors the preferred tools to quantify calcium levels. Consequently, developing ratiometric probes for other biologically important species has emerged as an important area of molecular design and synthesis.[6]

The zinc ion (Zn^{2+}) is one of the targets in the design of ratiometric probes, as this metal ion is of great interest in the field of neurobiology.[7] While Zn^{2+} is mostly trapped within proteins, as a structural or catalytic cofactor,[8] there is a pool of Zn^{2+} that is loosely bound or chelatable in the brain.[9] Especially in the hippocampus, a considerable amount of chelatable Zn^{2+} is accumulated in the synaptic vesicles of glutamatergic mossy fiber neurons, although its functional role remains unclear.[10] It is also known that disorder of Zn^{2+} metabolism is closely associated with many severe neurological diseases, including

† The University of Tokyo.
‡ CREST, Japan Science and Technology Agency.
§ PRESTO, Japan Science and Technology Agency.

(1) Tsien, R. Y. In *Fluorescent and Photochemical Probes of Dynamic Biochemical Signals Inside Living Cells*; Czarnik, A. W., Ed.; American Chemical Society: Washington, DC, 1993; pp 130−146.
(2) Mason, W. T. *Fluorescent and Luminescent Probes for Biological Activity*, 2nd ed.; Academic Press: New York, 1999.
(3) Grynkiewicz, G.; Poenie, M.; Tsien, R. Y. *J. Biol. Chem.* **1985**, *260*, 3440−3450.
(4) Tsien, R. Y. *Trends Neurosci.* **1988**, *11*, 419−424.
(5) Haugland, R. P. *Handbook of Fluorescent Probes and Research Products*, 10th ed.; Molecular Probes, Inc.: Eugene, OR, 2005.
(6) (a) Mizukami, S.; Nagano, T.; Urano, Y.; Odani, A.; Kikuchi, K. *J. Am. Chem. Soc.* **2002**, *24*, 3920−3925. (b) Maruyama, S.; Kikuchi, K.; Hirano, T.; Urano, Y.; Nagano, T. *J. Am. Chem. Soc.* **2002**, *124*, 10650−10651. (c) Kiyose, K.; Kojima, H.; Urano, Y.; Nagano, T. *J. Am. Chem. Soc.* **2006**, *128*, 6548−6549. (d) Takakusa, H.; Kikuchi, K.; Urano, Y.; Sakamoto, S.; Yamaguchi, K.; Nagano, T. *J. Am. Chem. Soc.* **2002**, *124*, 1653−1657. (e) Takakusa, H.; Kikuchi, K.; Urano, Y.; Kojima, H.; Nagano, T. *Chem.−Eur. J.* **2003**, *9*, 1479−1485. (f) Komatsu, T.; Kikuchi, K.; Takakusa, H.; Hanaoka, K.; Ueno, T.; Kamiya, M.; Urano, Y.; Nagano, T. *J. Am. Chem. Soc.* **2006**, *128*, 15946−15947.
(7) Frederickson, C. J.; Koh, J.-H.; Bush, A. I. *Nat. Neurosci.* **2005**, *6*, 449−462. (b) Chang, C. J.; Lippard, S. J. *Met. Ions Life Sci.* **2006**, *1*, 321−370.
(8) Vallee, B. L.; Falchuk, K. H. *Physiol. Rev.* **1993**, *73*, 79−118. (b) Berg, J. M.; Shi, Y. G. *Science* **1996**, *271*, 1081−1085.
(9) Frederickson, C. J. *Int. Rev. Neurobiol.* **1989**, *31*, 145−238.

Scheme 1. Synthesis of Iminocoumarins **3** and **4**

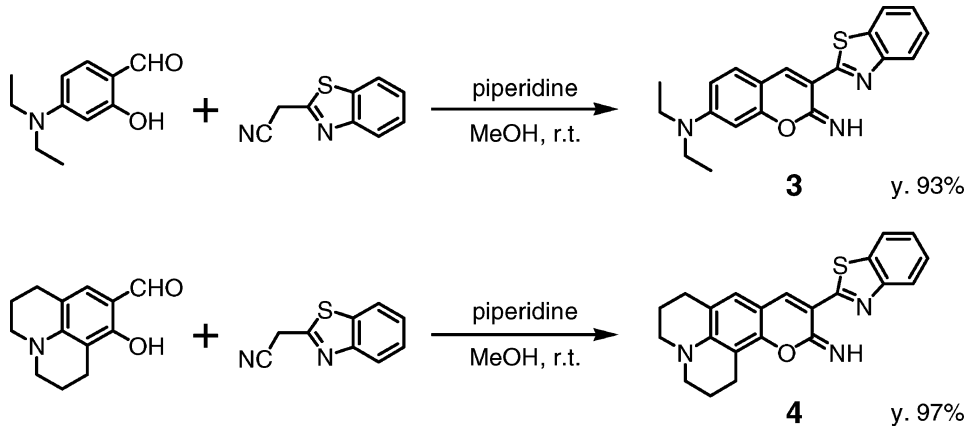

Alzheimer's disease (AD),[11] cerebral ischemia,[12] and epilepsy.[13] Therefore, measurement of Zn^{2+} is important in neurobiology.

In recent years, significant advances have been made in the design of fluorescence probes for Zn^{2+}.[14] Many intensity-based Zn^{2+} sensors are suitable for biological applications[15] and have been used with some success in Zn^{2+} neurobiology.[10h,15b,16] Protein-based[17] or peptide-based[18] strategies have also been employed. However, only a few ratiometric probes for Zn^{2+} have been reported[6b,c,15d,19] and have been applied in vivo.[6b,19b,c] Up to now, most studies concerning Zn^{2+} neurobiology have been carried out using hippocampal slices. In general, fluorescence imaging in hippocampal slices is relatively difficult, because the emission intensity is severely affected by factors such as the sample thickness and artifacts associated with the probe concentration and environment. Therefore, Zn^{2+} sensors suitable for fluorescence ratiometric imaging in hippocampal slices would have great value, because they would allow measurement of the Zn^{2+} concentration with greater precision. Currently developed ratiometric probes for Zn^{2+} are not satisfactory for microscopic imaging, because they require UV excitation, which can be damaging to cells and can cause interfering autofluorescence from native cellular species, or because of the low quantum yield of fluorescence in aqueous media. These features preclude facile application of these sensors for biological applications. Therefore, a sensor with superior photophysical properties is still required for ratiometric imaging of Zn^{2+} in biological applications.

In the present paper, we introduce iminocoumarin in the design of ratiometric probes for Zn^{2+}. Although coumarin derivatives are among the most widely studied fluorescent dyes, and probably the most widely used,[5,19e,20] very few investigations have been carried out on their 2-imino analogues, iminocoumarins, as a scaffold for fluorescence probes. In our exploration of iminocoumarin derivatives, we found that they have excellent photophysical properties and appear to be suitable for biological application. They are excited in the long wavelength range beyond 500 nm, and they have high fluorescence quantum yields in aqueous media. Furthermore, in contrast to coumarins, modification of the imino group allows facile synthesis of various derivatives, which is an important feature for the development of fluorescence probes. Here, we report the design, synthesis, and photophysical properties of a novel ratiometric probe for Zn^{2+}, using iminocoumarin as a fluorophore. We also

(10) (a) Frederickson, C. J.; Klitenick, M. A.; Manton, W. I.; Kirkpatrick, J. B. *Brain Res.* **1983**, *273*, 335−339. (b) Assaf, S. Y.; Chung, S. H. *Nature* **1984**, *308*, 734−736. (c) Howell, G. A.; Welch, M. G.; Frederickson, C. J. *Nature* **1984**, *308*, 736−738. (d) Li, Y.; Hough, C. J.; Frederickson, C. J.; Sarvey, J. M. *J. Neurosci.* **2001**, *21*, 8015−8025. (e) Li, Y.; Hough, C. J.; Suh, S. W.; Sarvey, J. M.; Frederickson, C. J. *J. Neurophysiol.* **2001**, *86*, 2597−2604. (f) Kay, A. R. *J. Neurosci.* **2003**, *23*, 6847−6855. (g) Qian, J.; Noebels, J. L. *J. Physiol.* **2005**, *566*, 747−758. (h) Frederickson, C. J.; Giblin, L. J.; Rengarajan, B.; Masalha, R.; Frederickson, C. J.; Zeng, Y.; Lopez, E. V.; Koh, J.-Y.; Chorin, U.; Besser, L.; Herskfinkel, M.; Li, Y.; Thompson, R. B.; Krezel, A. *J. Neurosci. Methods* **2006**, *154*, 19−29. (i) Kay, A. R. *Trends Neurosci.* **2006**, *29*, 200−206.

(11) Bush, A. I.; Pettingell, W. H.; Malthaup, G.; Paradis, M.; Vonsattel, J. P.; Gusella, J. F.; Beyreuther, K.; Masters, C. L.; Tanzi, R. E. *Science* **1994**, *265*, 1464−1467.

(12) Koh, J. Y.; Suh, S. W.; Gwag, B. J.; He, Y. Y.; Hsu, C. Y.; Choi, D. W. *Science* **1996**, *272*, 1013−1016.

(13) Frederickson, C. J.; Hernandez, M. D.; McGinty, J. F. *Brain Res.* **1989**, *480*, 317−321.

(14) (a) Kimura, E.; Koike, T. *Chem. Soc. Rev.* **1998**, *27*, 179−184. (b) Kikuchi, K.; Komatsu, K.; Nagano, T. *Curr. Opin. Chem. Biol.* **2004**, *8*, 182−191. (c) Jiang, P.; Guo, Z. *Coord. Chem. Rev.* **2004**, *248*, 205−229. (d) Lim, N. C.; Freake, H. C.; Bruckner, C. *Chem.*−*Eur. J.* **2005**, *11*, 38−49. (e) Carol, P.; Sreejith, S.; Ajayaghosh, A. *Chem. Asian J.* **2007**, *2*, 338−348.

(15) (a) Hirano, T.; Kikuchi, K.; Urano, Y.; Nagano, T. *J. Am. Chem. Soc.* **2002**, *124*, 6555−6562. (b) Komatsu, K.; Kikuchi, K.; Kojima, H.; Urano, Y.; Nagano, T. *J. Am. Chem. Soc.* **2005**, *127*, 10197−10204. (c) Gee, K. R.; Zhou, Z.-L.; Qian, W.-J.; Kennedy, R. *J. Am. Chem. Soc.* **2002**, *124*, 776−778. (d) Gee, K. R.; Zhou, Z.-L.; Ton-That, D.; Sensi, S. L.; Weiss, J. H. *Cell. Calcium* **2002**, *31*, 245−251. (e) Burdette, S. C.; Walkup, G. K.; Spingler, B.; Tsien, R. Y.; Lippard, S. J. *J. Am. Chem. Soc.* **2001**, *123*, 7831−7841. (f) Burdette, S. C.; Frederickson, C. J.; Bu, W.; Lippard, S. J. *J. Am. Chem. Soc.* **2003**, *125*, 1778−1787. (g) Chang, C. J.; Nolan, E. M.; Jaworski, J.; Burdette, S. C.; Sheng, M.; Lippard, S. J. *Chem. Biol.* **2004**, *11*, 203−210. (h) Nolan, E. M.; Jaworski, J.; Okamoto, K.-I.; Hayashi, Y.; Sheng, M.; Lippard, S. J. *J. Am. Chem. Soc.* **2005**, *127*, 16812−16823. (i) Nolan, E. M.; Jaworski, J.; Racine, M. E.; Sheng, M.; Lippard, S. J. *Inorg. Chem.* **2006**, *45*, 9748−9757. (j) Nolan, E. M.; Ryu, J. W.; Jaworski, J.; Feazell, R. P.; Sheng, M.; Lippard, S. J. *J. Am. Chem. Soc.* **2006**, *128*, 15517−15528. (k) Tang, B.; Huang, H.; Xu, K. H.; Tong, L. L.; Yang, G. W.; Liu, X.; An, L. G. *Chem. Commun.* **2006**, 3609−3611.

(16) (a) Ueno, S.; Tsukamoto, M.; Hirano, T.; Kikuchi, K.; Yamada, M. K.; Nishiyama, N.; Nagano, T.; Matsuki, N.; Ikegaya, Y. *J. Cell Biol.* **2002**, *158*, 215−220. (b) Qian, J.; Noebels, J. L. *J. Physiol.* **2005**, *566*, 747−758.

(17) (a) Thompson, R. B.; Maliwal, B. P. *Anal. Chem.* **1998**, *70*, 1749−1754. (b) Thompson, R. B.; Whetsell, W. O.; Maliwal, B. P.; Fierke, C. A.; Frederickson, C. J. *J. Neurosci. Methods* **2000**, *96*, 35−45. (c) Thompson, R. B.; Cramer, M. L.; Bozym, R. *J. Biomed. Opt.* **2002**, *7*, 555−560. (d) Bozym, R. A.; Thompson, R. B.; Stoddard, A. K.; Fierke, C. A. *ACS Chem. Biol.* **2006**, *1*, 103−111. (e) Van Dongen, E.; Dekkers, L. M.; Spijker, K.; Meijer, E. W.; Klomp, L. W. J.; Merkx, M. *J. Am. Chem. Soc.* **2006**, *128*, 10754−10762.

(18) (a) Godwin, H. A.; Berg, J. M. *J. Am. Chem. Soc.* **1996**, *118*, 6514−6515. (b) Walkup, G. K.; Imperiali, B. *J. Am. Chem. Soc.* **1996**, *118*, 3053−3054. (c) Shults, M. D.; Pearce, D. A.; Imperiali, B. *J. Am. Chem. Soc.* **2003**, *125*, 10591−10597.

(19) (a) Woodroofe, C. C.; Lippard, S. J. *J. Am. Chem. Soc.* **2003**, *125*, 11458−11459. (b) Taki, M.; Wolford, J. L.; O'Halloran, T. V. *J. Am. Chem. Soc.* **2004**, *126*, 712−713. (c) Chang, C. J.; Jaworski, J.; Nolan, E. M.; Sheng, M.; Lippard, S. J. *Proc. Natl. Acad. Sci. U.S.A.* **2004**, *101*, 1129−1134. (d) Henary, M. M.; Wu, Y.; Fahrni, C. J. *Chem.*−*Eur. J.* **2004**, *10*, 3015−3025. (e) Lim, N. C.; Schuster, J. V.; Porto, M. C.; Tanudra, M. A.; Yao, L. L.; Freake, H. C.; Bruckner, C. *Inorg. Chem.* **2005**, *44*, 2018−2030. (f) Ajayaghosh, A.; Carol, P.; Sreejith, S. *J. Am. Chem. Soc.* **2005**, *127*, 14962−14963. (g) Mei, Y. J.; Bentley, P. A. *Bioorg. Med. Chem. Lett.* **2006**, *16*, 3131−3134.

(20) Katerinopoulos, H. E. *Curr. Pharm. Des.* **2004**, *10*, 3835−3852.

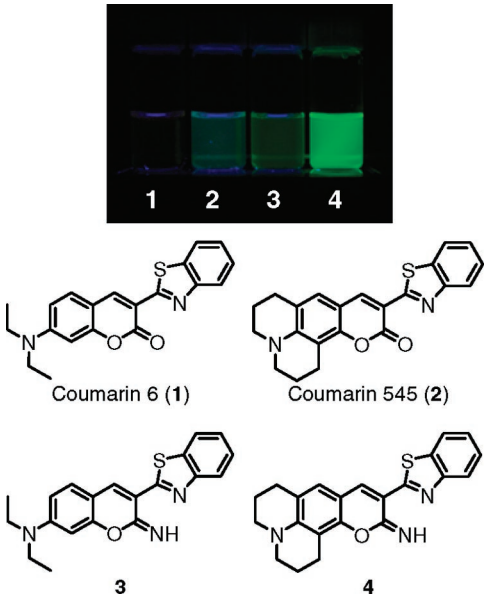

Figure 1. Evaluation of iminocoumarins as a scaffold for fluorescence probes: (top) photograph of the fluorescence of coumarin 6 (**1**), coumarin 545 (**2**), **3**, and **4**; (bottom) structures of the coumarin−benzothiazole derivatives. Each sample was prepared in 100 mM sodium phosphate buffer (pH 7.4), containing less than 0.25% DMSO as a cosolvent.

Table 1. Photochemical Properties of Coumarin−Benzothiazole Derivatives[a]

dye	absorption λ_{max} (nm)	extinction coeff ϵ [b] ($M^{-1}cm^{-1}$)	emission λ_{max} (nm)	quantum yield[c]
coumarin 6 (**1**)	492	1.5×10^4	520	0.08
coumarin 545 (**2**)	467	2.5×10^4	530	0.10
3	487	2.8×10^4	524	0.07
4	503	3.2×10^4	537	0.63

[a] All data were obtained at pH 7.4 in 100 mM sodium phosphate buffer, containing less than 0.25% DMSO as a cosolvent. [b] Measured at each absorption λ_{max}. [c] Quantum yields of fluorescence were determined by using that of fluorescein (0.85) in 0.1 N NaOH as a standard.[22]

present applications of this probe to measure Zn^{2+} concentrations in cultured cells and in rat hippocampal slices.

Results and Discussion

Evaluation of Iminocoumarins as a Scaffold for Fluorescence Probes. In our search for new fluorophores suitable for ratiometric imaging, we first prepared four coumarin and iminocoumarin derivatives and examined their fluorescence properties in pH-buffered aqueous solutions. Iminocoumarins **3** and **4** were synthesized according to Scheme 1. As shown in Figure 1 and Table 1, we unexpectedly found that only **4** showed strong fluorescence with a large extinction coefficient and high fluorescence quantum yield. It also exhibited a long excitation wavelength (503 nm). On the other hand, coumarin 6 (**1**) showed quite weak fluorescence, although a **1**-based sensor, BTC, is now commercially available and widely used for ratiometric imaging of Ca^{2+}. These findings clearly indicate that **4** is a good candidate as a fluorophore for ratiometric probes. This is an interesting result, because many coumarin derivatives have been investigated as scaffolds for fluorescence probes for biological applications, but most of them are not suitable for microscopic imaging because of the need for UV excitation or the low fluorescence quantum yield in aqueous media. We believe this finding provides the basis for a new design strategy for fluorescence probes.

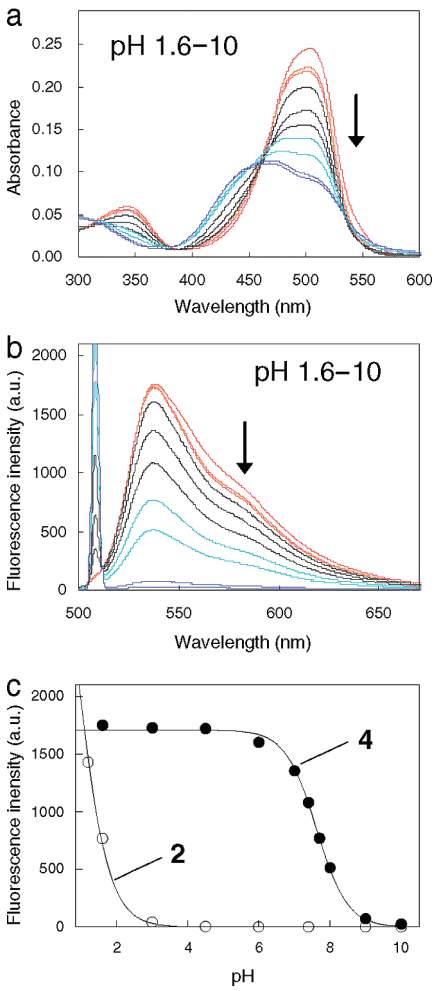

Figure 2. Effect of pH on the fluorescence properties of iminocoumarin **4**. Absorption (a) and fluorescence (b) spectra of 5 μM **4** were measured in 100 mM sodium phosphate buffer at various pH values (pH 1.6−10). (c) shows the fluorescence intensity versus pH for iminocoumarin **4** (closed circles) and its coumarin analogue **2** (open circles). The fluorescence intensity of **4** (excitation 508 nm, emission 537 nm) or **2** (excitation 540 nm, emission 562 nm) was measured in 100 mM sodium phosphate buffer.

Effect of pH on the Fluorescence Properties of the Iminocoumarin 4. We next investigated the effect of pH on the fluorescence properties of the iminocoumarin **4** to understand the reason for its excellent characteristics. The absorption and fluorescence spectra of **4** are shown in Figure 2a,b. Compound **4** showed strong fluorescence in acidic and neutral solutions, but had little fluorescence in basic solutions. This pH profile was not observed in the case of the coumarin analogue coumarin 545 (**2**), which showed little fluorescence over a wide pH region, except in strong acids (Figure 2c). There is no structural difference between these two dyes apart from the 2-substituted atoms. Therefore, it seems likely that the imino nitrogen must be protonated for **4** to show strong fluorescence and that the deprotonated form has little fluorescence, like **2**. These results establish the pH-dependent fluorescence intensity of iminocoumarin **4** in the neutral and basic regions. However, its emission wavelength was not dependent on pH. Therefore, the fluorescence intensity ratio remains constant over a wide pH range (discussed in more detail later).

Design and Synthesis of a Ratiometric Probe for Zn^{2+}. Another significant advantage of iminocoumarins over cou-

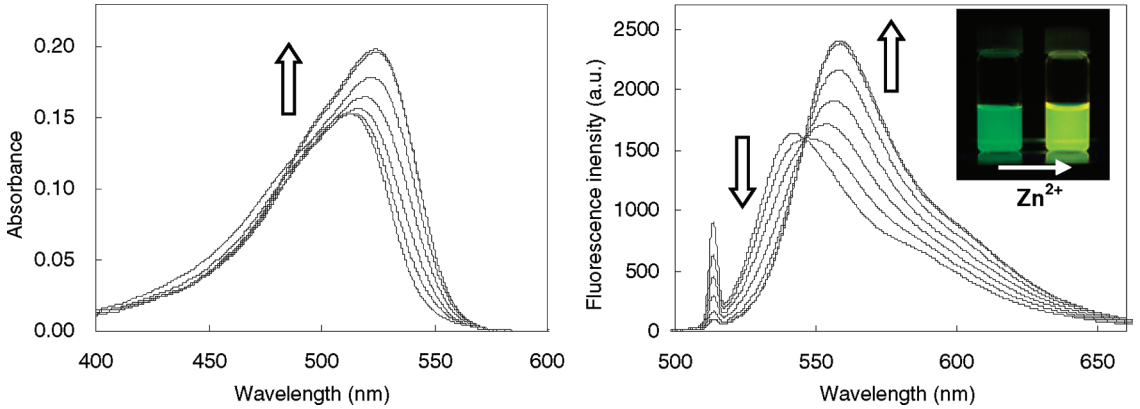

Figure 3. Absorption (left) and emission (right) spectra of 5 μM ZnIC in the presence of various concentrations of Zn^{2+}: 0, 0.2, 0.4, 0.6, 0.8, 1.0, and 2.0 equiv of Zn^{2+} with respect to [ZnIC]. These spectra were measured at pH 7.4 in 100 mM HEPES buffer, $I = 0.1$ ($NaNO_3$), containing 0.25% DMSO as a cosolvent. The excitation wavelength was 513 nm. Inset: red shift of the fluorescence emission of 20 μM ZnIC in the absence ($-Zn^{2+}$) or presence ($+Zn^{2+}$) of 100 μM Zn^{2+}.

Scheme 2. Synthesis of ZnIC

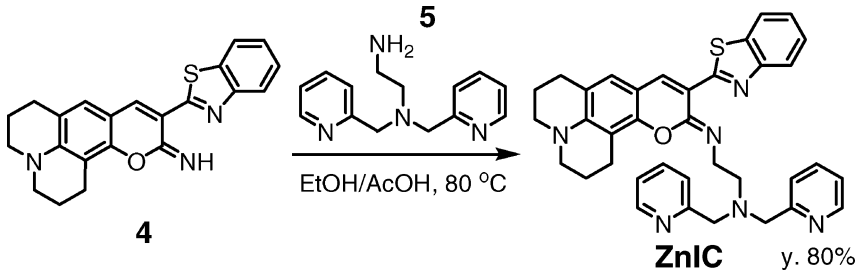

marins is the facile synthesis of derivatives by modification of the imino function. To develop a Zn^{2+} sensor for ratiometric measurement, we newly designed and synthesized ZnIC (Scheme 2) using this strategy. The Zn^{2+}-chelating moiety *N*,*N*-bis(2-pyridylmethyl)ethanediamine (**5**) was synthesized following a literature procedure.[23] ZnIC was easily synthesized in one step in high yield, by conjugating **4** with **5**.

Spectroscopic Properties of ZnIC and Optical Responses to Zn^{2+}. The characteristics of ZnIC were evaluated at physiological ionic strength and pH (100 mM HEPES, pH 7.4, $I = 0.1$ ($NaNO_3$)). This iminocoumarin-based sensor exhibits absorption bands in the visible region centered at 513 nm ($\epsilon = 3.9 \times 10^4$ M^{-1} cm^{-1}). Upon excitation at 513 nm, an emission spectrum with a maximum at 543 nm was observed. The quantum yield of fluorescence for the metal-free ligand ZnIC is 0.80. The absorption and emission profiles of ZnIC resemble those of **4**, indicating that this derivative retains the favorable fluorescence properties of the iminocoumarin.

Coordination of Zn^{2+} to ZnIC led to striking changes in the emission color (Figure 3). The observed changes in absorption and emission spectra occur up to a 1/1 [Zn^{2+}]/[ZnIC] ratio, indicating the formation of a 1/1 complex. Upon addition of Zn^{2+}, the visible absorption profile of ZnIC red shifts to a peak centered at 524 nm ($\epsilon = 3.9 \times 10^4$ M^{-1} cm^{-1}). Excitation at 513 nm produces a fluorescence spectrum centered at 558 nm. The quantum yield of fluorescence for the Zn^{2+}−ZnIC complex is 0.76. Taken together, these data establish that ZnIC functions as a single-excitation, dual-emission ratiometric probe for Zn^{2+} that exhibits strong fluorescence in aqueous media with visible light excitation. The ratio of emission intensities F_{558}/F_{543} upon excitation at 513 nm varies from 0.8 in the absence of Zn^{2+} to 1.9 in the presence of equimolar Zn^{2+}.

The red shift in the emission of ZnIC after Zn^{2+} coordination can be explained in terms of the intramolecular charge transfer (ICT) mechanism.[24] When a fluorophore contains an electron-donating group (often an amino group) conjugated to an electron-withdrawing group, it undergoes ICT from the donor to the acceptor upon excitation by light. The consequent change of the dipole moment leads to a larger Stokes shift, which is influenced by the microenvironment of the fluorophore. Therefore, when a cation such as Zn^{2+} interacts with the acceptor group, the excited state is more stabilized by the cation than is the ground state, and this leads to a red shift of the absorption and emission spectra. This mechanism is quite general, and therefore, we can reasonably expect to develop many sensors directed to other targets by employing iminocoumarin as a fluorophore.

Binding Affinity for Zn^{2+}. Fluorescence spectroscopy was used to determine the apparent Zn^{2+} complex K_d values for ZnIC, using Zn^{2+} and pH-buffered solutions[25] (Figure 4). ZnIC responds to picomolar concentrations of free ionic Zn^{2+}, and binding of Zn^{2+} to the probe was monitored by measuring the

(21) (a) Liepouri, F.; Foukaraki, E.; Deligeorgiev, T. G.; Katerinopoulos, H. E. *Cell. Calcium* **2001**, *30*, 331−335. (b) Liepouri, F.; Deligeorgiev, T. G.; Veneti, Z.; Savakis, C.; Katerinopoulos, H. E. *Cell. Calcium* **2002**, *31*, 221−227. (c) Roussakis, E.; Liepouri, F.; Nifli, A. P.; Castanas, E.; Deligeorgiev, T. G.; Katerinopoulos, H. E. *Cell. Calcium* **2006**, *39*, 3−11.
(22) Paeker, C. A.; Rees, W. T. *Analyst* **1960**, *85*, 587−600.
(23) Kawabata, E.; Kikuchi, K.; Urano, Y.; Kojima, H.; Odani, A.; Nagano, T. *J. Am. Chem. Soc.* **2005**, *127*, 818−819.
(24) Valeur, B.; Leray, I. *Coord. Chem. Rev.* **2000**, *205*, 3−40.
(25) (a) Fahrni, C. J.; O'Halloran, T. V. *J. Am. Chem. Soc.* **1999**, *121*, 11448−11458. (b) Hirano, T.; Kikuchi, K.; Urano, Y.; Higuchi, T.; Nagano, T. *J. Am. Chem. Soc.* **2000**, *122*, 12399−12400.

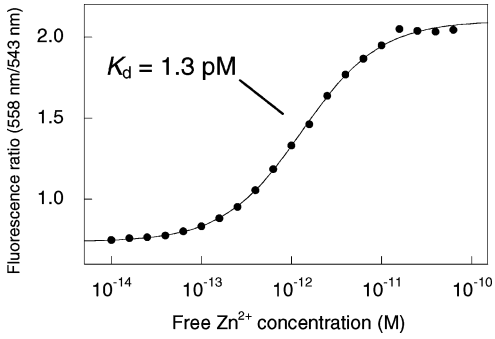

Figure 4. Fluorescence ratio of 5 μM ZnIC as a function of the concentration of free Zn^{2+} in 100 mM HEPES buffer (pH 7.4, $I = 0.1$ ($NaNO_3$)) with 10 mM HEDTA and 0−9.4 mM Zn^{2+}. All data are expressed as the fluorescence ratio (558 nm/543 nm). These data were fitted to eq 2 in the Experimental Section, and K_d was calculated. The excitation wavelength was 513 nm.

ratio of fluorescence intensities collected at 543 and 558 nm. This analysis provided an apparent K_d value of 1.3 pM for the 1/1 complex. This value is very much smaller than those of previously reported Zn^{2+} fluorescence probes. We previously reported that Zn^{2+} concentrations vary drastically around the nanomolar level in biological samples, especially in the brain.[15b] Therefore, ZnIC is sufficiently sensitive for use in biological applications.

Metal Ion Selectivity. The titration of ZnIC with various metal ions was conducted to examine the selectivity (Figure 5). The fluorescence of ZnIC was not influenced by other cations, such as Ca^{2+}, Mg^{2+}, Na^+, and K^+, which exist at high concentration under physiological conditions, even at as high a concentration as 5 mM. Thus, this molecule can be used even under biological conditions involving an increase of Ca^{2+} concentration. However, Cd^{2+} shifted the ZnIC spectrum in the same way as Zn^{2+}. Fe^{2+}, Co^{2+}, and Cu^{2+} formed complexes with ZnIC and strongly quenched the fluorescence of this molecule, but these free cations would have little influence in vivo, since they exist at very low concentrations.[26]

Effect of pH on the Fluorescence Ratio. The influence of pH on the fluorescence ratio of ZnIC was also examined. The metal-free ligand of ZnIC had a pH profile similar to that of **4**, and its fluorescence was quenched in basic solutions. However, the ratio of the two fluorescence intensities remained constant. On the other hand, no change in fluorescence intensity was observed in the ZnIC−Zn^{2+} complex over a wide pH range. The calculated fluorescence ratio F_{558}/F_{543} indicates that ZnIC can detect Zn^{2+} independently of pH in the pH range of 3−9 (Figure 6).

Biological Application of ZnIC to Cultured Cells. We next examined the application of ZnIC for ratiometric fluorescence imaging of Zn^{2+} in cultured living cells (HEK cells). Following incubation with DMEM containing 10 μM ZnIC at room temperature for 30 min, the cells were stained, indicating that ZnIC can permeate into the cells and accumulate in them. Ratiometric fluorescence imaging of ZnIC-stained cells was performed by using two emission filters (565−605 and 510−550 nm). The ratio of fluorescence intensities at 565−605 and 510−550 nm increased immediately upon addition of Zn^{2+} and 2-mercaptopyridine *N*-oxide (pyrithione), which is a zinc-selective ionophore, to the medium. Treatment of the cells with the membrane-permeable metal ion chelator TPEN reversed the fluorescence ratio enhancements to baseline levels (Figure 7), which confirms that the increase in fluorescence ratio results from Zn^{2+} coordination and not from other phenomena, such as proton flux or sensor photoactivation. These experiments indicate that ZnIC is an effective ratiometric probe for biological applications and can reversibly monitor changes in intracellular Zn^{2+}.

Ratiometric Detection of Zn^{2+} in Live Hippocampal Slices. We next examined the usefulness of ZnIC to detect endogenous Zn^{2+} pools. We therefore treated acute hippocampal slices from adult rat brain with 20 μM ZnIC for 1.5 h at room temperature for dye loading. Figure 8a−d shows the results of fluorescence imaging of a representative dye-loaded slice. The fluorescence images with emission collected at 565−605 and 510−550 nm both have regions of intense fluorescence, which seemed to be derived from localization of the dye. However, this effect was diminished in the ratio image, and higher ratios were clearly observed in the dentate gyrus, CA3, and CA1 regions, which contain glutamatergic neurons rich in vesicular zinc. These ratiometric signals disappeared upon addition of TPEN, indicating that ZnIC can detect endogenous Zn^{2+} in these regions. To our knowledge, this is the first example of ratiometric fluorescence imaging to visualize endogenous Zn^{2+} in hippocampal slices. As compared with that in cultured cells, the fluorescence intensity in hippocampal slices is severely affected by factors such as the sample thickness and artifacts associated with the probe concentration and environment. Therefore, intensity-based

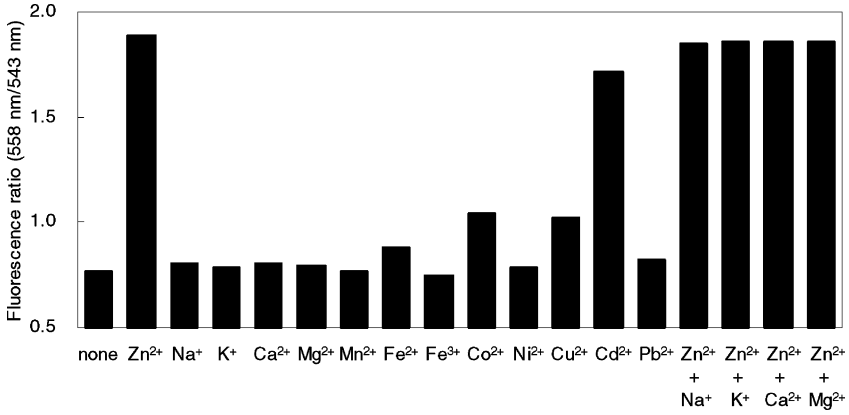

Figure 5. Metal ion selectivity of ZnIC. All data were obtained at pH 7.4 (100 mM HEPES buffer, $I = 0.1$ ($NaNO_3$)) and are expressed as the fluorescence ratio (558 nm/543 nm). The excitation wavelength was 513 nm. Zn^{2+}, Mn^{2+}, Fe^{2+}, Fe^{3+}, Co^{2+}, Ni^{2+}, Cu^{2+}, Cd^{2+}, and Pb^{2+} (10 μM) and Na^+, K^+, Ca^{2+}, and Mg^{2+} (5 mM) were added to 5 μM ZnIC.

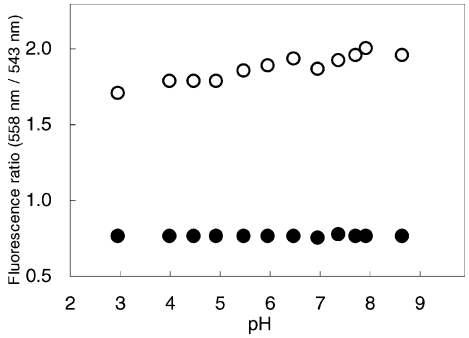

Figure 6. Effect of pH on the fluorescence ratio F_{558}/F_{543} of 5 μM ZnIC in the absence (closed circles) or presence (open circles) of 100 μM Zn^{2+}. All data were obtained at various pH values (pH 3−9) in the presence of 0.25% DMSO as a cosolvent and are expressed as the fluorescence ratio (558 nm/543 nm). The excitation wavelength was 513 nm.

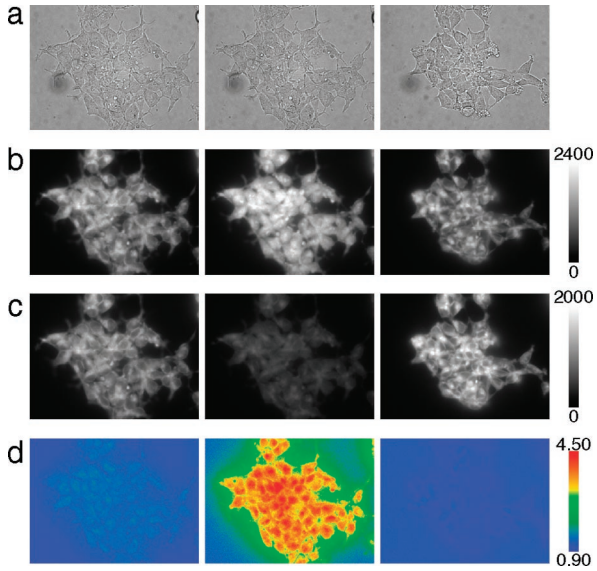

Figure 7. Fluorescence ratiometric imaging of intracellular Zn^{2+} using ZnIC. HEK293 cells incubated with 10 μM ZnIC for 30 min at room temperature were washed with DMEM (left), ZnIC-stained cells were exposed to 10 μM pyrithione and 50 μM Zn^{2+} for 5 min (middle), and return of intracellular Zn^{2+} to the resting level was achieved by addition of 300 μM TPEN (right). Fluorescence images were acquired with excitation at 480−500 nm. (a) Bright-field transmission images. (b) Fluorescence images with emission collected at 565−605 nm. (c) Fluorescence images with emission collected at 510−550 nm. (d) Ratiometric images generated from (b) and (c).

probes for Zn^{2+} sometimes fail to stain endogenous Zn^{2+}, as shown in Figure 8e (right), depending on even minor differences of sample preparation or other factors within the same protocol. On the other hand, ratiometric measurement is expected to overcome such problems and to afford clear and stable images, because the ratio between two fluorescence intensities is independent of such factors. This indeed appears to be the case with our newly developed ratiometric probe ZnIC. For example, the intense fluorescence on the left lower side of Figure 8b,c was clearly canceled out in the ratiometric image of Figure 8d. Furthermore, the fluorescence intensity of the intensity-based probe for Zn^{2+}, ZnAF-2, gradually decreased during the time course measurement, while the fluorescence ratio of ZnIC was

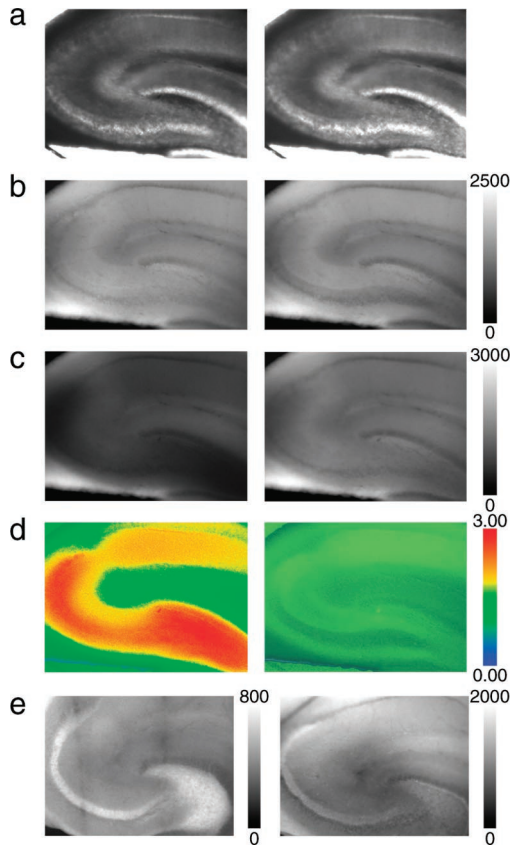

Figure 8. Fluorescence ratiometric imaging of Zn^{2+} in a rat hippocampal slice with ZnIC. The slice was incubated with 20 μM ZnIC containing 0.01% Cremophore and 1% DMSO for 1.5 h at room temperature and then washed with ACSF for 0.5 h. Bright-field and fluorescence images excited at 480−500 nm were acquired (left) before and (right) after incubation with 300 μM TPEN for 0.5 h at room temperature. (a) Bright-field transmission images. (b) Fluorescence images with emission collected at 565−605 nm. (c) Fluorescence images with emission collected at 510−550 nm. (d) Ratiometric images generated from (b) and (c). (e) Two examples of application of an intensity-based Zn^{2+} sensor, ZnAF-2, to hippocampal slices, showing different Zn^{2+} staining patterns.

stable (data not shown). We believe these advantages of ratiometric measurement will be of great value in investigations of the biological significance of Zn^{2+}.

Conclusion

We examined various coumarin and iminocoumarin derivatives which are excitable with visible light and found that the iminocoumarin **4** showed much stronger fluorescence than its coumarin analogue. We utilized these findings to develop an iminocoumarin-based probe, ZnIC, suitable for ratiometric imaging of intracellular Zn^{2+}. ZnIC allows single-excitation, dual-emission ratiometric sensing of Zn^{2+} through the intramolecular charge-transfer mechanism. ZnIC is selective for Zn^{2+} over biologically competing alkali- and alkaline-earth-metal ions, and its long-wavelength visible excitation and emission profiles are expected to minimize cell and tissue damage, while also avoiding interfering autofluorescence from native cellular species. ZnIC was confirmed to be directly applicable to monitor changes in intracellular Zn^{2+} in living cells, owing to its membrane permeability. Ratiometric imaging with ZnIC could clearly visualize endogenous Zn^{2+} in hippocampal slices without suffering from dye localization artifacts.

(26) Rae, T. D.; Schmidt, P. J.; Pufahl, R. A.; Culotta, V. C.; O'Halloran, T. V. *Science* **1999**, *284*, 805−808.

Experimental Section

Materials and General Instrumentation. All reagents and solvents were of the highest commercial quality and were used without purification, except for *N*,*N*-dimethylformamide, ethanol, and dichloromethane, which were used after distillation. Dimethyl sulfoxide (DMSO), 2-[4-(2-hydroxyethyl)-1-piperazinyl]ethanesulfonic acid (HEPES), *N*-(2-hydroxyethyl)ethylenediamine-*N*,*N*′,*N*′-triacetic acid (HEDTA), *N*,*N*,*N*′,*N*′-tetrakis(2-pyridylmethyl)ethylenediamine (TPEN), 2-morpholinoethanesulfonic acid (MES), and *N*-cyclohexyl-2-aminoethanesulfonic acid (CHES) were purchased from Dojindo Laboratories, Ltd. (Kumamoto, Japan). 3-(2-Benzothiazolyl)-7-(diethylamino)coumarin (coumarin 6 (**1**)) was purchased from Tokyo Chemical Industry Co. Ltd. (Tokyo, Japan). 10-(1,3-Benzothiazol-2-yl)-2,3,6,7-tetrahydro-1*H*,5*H*,11*H*-[1]benzopyrano[6,7,8-*ij*]quinoliz-11-one (coumarin 545 (**2**))[27] and **5**[23] were prepared according to the literature, and the purity of these compounds was checked by ^{1}H NMR spectroscopy. All other reagents were purchased from Tokyo Chemical Industry Co. Ltd., Wako Pure Chemical Industries, Ltd. (Osaka, Japan), or Aldrich Chemical Co. Inc. (Milwaukee, WI). NMR spectra were recorded on a JNM-LA300 (JEOL Ltd., Tokyo, Japan) instrument at 300 MHz for ^{1}H NMR and at 75 MHz for ^{13}C NMR. δ values are given in parts per million relative to the peak for tetramethylsilane. Mass spectra were measured with a JEOL JMS-T100LC AccuTOF (ESI$^+$). Silica gel column chromatography was performed using BW-300, Chromatorex-NH (Fuji Silysia Chemical Ltd., Kasugai, Japan), or silica gel 60N (Kanto Chemical Co. Inc., Tokyo, Japan).

Measurement of Photochemical Properties. UV−vis spectra were measured using an ultraviolet−visible spectrophotometer, UV-1600 (Shimadzu Corp., Kyoto, Japan). Fluorescence spectroscopic studies were performed with a Hitachi F4500 fluorescence spectrophotometer (Hitachi, Ltd., Tokyo, Japan). The slit width was 2.5 nm for both excitation and emission. The photomultiplier voltage was 750 V. All experiments were carried out at 298 K, unless otherwise specified. For absorption or fluorescence measurements, compounds were dissolved in DMSO to obtain stock solutions (2−10 mM). These stock solutions were diluted with buffer as specified in the figure captions to the desired concentration. For the determination of the quantum efficiency of fluorescence (Φ_{fl}), fluorescein in 0.1 M NaOH ($\Phi_{fl} = 0.85$) was used as a fluorescence standard.[22]

Preparation of Zn^{2+} and pH-Buffered Solutions. We prepared 100 mM HEPES buffer (pH 7.4, $I = 0.1$ ($NaNO_3$)) including 10 mM HEDTA and 0−9.4 mM $ZnSO_4$. The stability constant for the Zn^{2+} complex of HEDTA was taken from the literature.[28] Thus, for HEDTA, $pK_1 = 9.87$, $pK_2 = 5.38$, $pK_3 = 2.62$, and $\log K(ZnL) = 14.6$ (25 °C, $I = 0.1$). Protonation constants must be corrected upward by 0.11 when working at 0.1 M ionic strength.[25a] Using these values, the free Zn^{2+} concentration was calculated using the reported method.[29] Thus

$$[Zn^{2+}]_{free} = [Zn^{2+}]_{total}/[K(ZnL)]\alpha_M[L]_{free} \quad (1)$$

$$\alpha_M = 1 + 10^{pH-pK_{a1}} + 10^{2pH-pK_{a1}-pK_{a2}} + 10^{3pH-pK_{a1}-pK_{a2}-pK_{a3}}$$

$$[L]_{free} \approx [L]_{total} - [Zn^{2+}]_{total}$$

$[L]_{total}$ was set at 10 mM, and $[Zn^{2+}]_{total}$ was varied from 0 to 9.4 mM. The value of $[Zn^{2+}]_{free}$ was obtained from eq 1 (see Table 2).

Determination of the Apparent Dissociation Constant (K_d) with Zn^{2+}. The fluorescence ratio F_{558}/F_{543} of 5 μM ZnIC excited at 513 nm as a function of the concentration of free Zn^{2+} was measured in 100 mM HEPES buffer (pH 7.4, $I = 0.1$, ($NaNO_3$)) including 10 mM HEDTA and 0−9.4 mM $ZnSO_4$. These data were fitted to eq 2, and K_d was calculated, where F is the fluorescence intensity, F_{max} is the maximum fluorescence intensity, F_0 is the fluorescence intensity with no addition of Zn^{2+}, and $[Zn^{2+}]_{free}$ is the free Zn^{2+} concentration.

Table 2

$[Zn^{2+}]_{total}$ (mM)	0.10	0.25	0.59	1.4	2.8	5.0	7.2	8.6	9.4
$[Zn^{2+}]_{free}$ (pM)	0.010	0.025	0.063	0.16	0.40	1.0	2.5	6.3	16

$$F = F_0 + (F_{max} - F_0)\,([Zn^{2+}]_{free})/(K_d + [Zn^{2+}]_{free}) \quad (2)$$

Metal Ion Selectivity Measurement. The fluorescence ratio F_{558}/F_{543} of 5 μM ZnIC excited at 513 nm was measured in 100 mM HEPES buffer (pH 7.4, $I = 0.1$ ($NaNO_3$)). The following heavy metal ions (10 μM) were added: $ZnSO_4$, $MnSO_4$, $FeSO_4$, $Fe_2(SO_4)_3$, $CoSO_4$, $NiSO_4$, $CuSO_4$, $CdSO_4$, and $Pb(NO_3)_2$. Other metal ions were added at 5 mM: NaCl, KCl, $CaCl_2$, and $MgSO_4$.

Effect of pH on the Fluorescence Ratio. The following buffers were used: 100 mM $ClCH_2COOH$−$ClCH_2COONa$ buffer (pH 3.0), 100 mM AcOH−AcONa buffer (pH 4.0−5.0), 100 mM MES buffer (pH 5.5−6.5), 100 mM HEPES buffer (pH 7.0−8.0), and 100 mM CHES buffer (pH 8.5−9.0). The fluorescence ratio F_{558}/F_{543} of 5 μM ZnIC excited at 513 nm diluted with these buffers in the absence or presence of 100 μM Zn^{2+} was measured.

Ratiometric Imaging System. The ratiometric imaging system comprised an inverted microscope (IX71; Olympus Corp., Tokyo, Japan) and a cooled CCD camera (Cool Snap HQ; Roper Scientific, Tucson, AZ). The microscope was equipped with a xenon lamp (AH2-RX, Olympus), an objective lens for HEK cells (Uapo/340 40×/1.35, Olympus) or for hippocampal slices (UPlanAPo 4×/0.16, Olympus), a dichroic mirror (FF506-Di02-25; Semrock, Inc., Rochester, NY), an excitation filter (S490/20×; Chroma Technology Corp., Brattleboro, VT), and two emission filters (S528/328, Chroma; FF555-E02-25, Semrock). The whole system was controlled with MetaFluor 6.1 software (Universal Imaging, Media, PA). For fluorescence imaging with the intensity-based Zn^{2+} probe ZnAF-2, we used the same imaging system, but with a different excitation filter (BP470-490, Olympus), dichroic mirror (DM505, Olympus), and emission filter (BA510-550, Olympus).

Preparation of Cells. HEK 293 cells were cultured in Dulbecco's modified Eagle's medium (DMEM) (Invitrogen Corp., Carlsbad, CA), supplemented with 10% fetal bovine serum (Invitrogen), 1% MEM nonessential amino acid solution (Invitrogen), and 2 mM glutamine (Invitrogen) at 37 °C in a 5/95 CO_2/air incubator. The cells were passaged 3 days before dye loading on an uncoated 35 mm diameter glass-bottomed dish (MatTek Corp., Ashland, MA). Then the cells were rinsed with DMEM, incubated with DMEM containing 10 μM ZnIC for 30 min at 37 °C, washed with DMEM twice, and mounted on the microscope stage.

Preparation of Rat Hippocampal Slices. The whole brains of adult Wistar rats (male, 200−250 g) were removed quickly under ether anesthesia and placed in ice-cold ACSF (artificial cerebrospinal fluid), which was aerated with 95/5 O_2/CO_2. The composition of ACSF was 124 mM NaCl, 2.5 mM KCl, 26 mM $NaHCO_3$, 1.25 mM NaH_2PO_4, 2.0 mM $CaCl_2$, 1.0 mM $MgCl_2$, and 10 mM glucose. The hippocampus was isolated, placed on an agar plate, and sliced into 300 μm thick slices with a rotary slicer (model DTY 7700; Dosaka EM Co. Ltd., Kyoto, Japan). The fresh hippocampal slices were incubated in ACSF equilibrated with 95/5 O_2/CO_2 for more than 30 min at room temperature. Then they were loaded with 20 μM ZnIC containing 0.01% Cremophore or 10 μM ZnAF-2 DA for 1.5 h at room temperature. A small flow-through chamber, whose base consisted of a thin glass coverslip, was placed on a microscopic stage. Then a dye-loaded slice was placed in the chamber and incubated or continuously perfused (2.5

(27) Khilya, O. V.; Frasinyuk, M. S.; Turov, A. V.; Khilya, V. P. *Chem. Heterocycl. Compd.* **2001**, *37*, 1029−1037.
(28) Martell, A. E.; Smith, R. M. NIST Critical Stability Constants of Metal Complexes. *NIST Standard Reference Database 46*, version 5.0; National Institute of Standards and Technology: Gaithersburg, MD, 1998.
(29) Perrin, D. D.; Dempsey, B. *Buffers for pH and Metal Ion Control*; John Wiley & Sons, Chapman and Hall: New York, London, 1974.

mL/min) with equilibrated ACSF at 33−34 °C. The slice was held in place by a metal wire ring with a stretched nylon net.

Preparation of 3. To a solution of 2-benzothiazoleacetonitrile (0.55 g, 2.8 mmol) in 50 mL of dry methanol was added piperidine (2.8 mL, 28 mmol), and the solution was stirred at room temperature for 3 min. Then 4-(diethylamino)salicylaldehyde (0.49 g, 2.8 mmol) was added. The mixture was stirred for 5 h at room temperature, and the precipitate was collected by filtration, washed with dry methanol, and dried under high vacuum to afford **3** (0.92 g, 93%). ^{1}H NMR (300 MHz, $CDCl_3$): δ 8.13 (br, 1H), 7.98 (d, 1H, J = 7.7 Hz), 7.85 (d, 1H, J = 7.7 Hz), 7.47−7.40 (m, 1H), 7.34−7.28 (m, 1H), 7.19 (d, 1H, J = 8.8 Hz), 6.40 (dd, 1H, J = 8.8, 2.3 Hz), 6.32 (d, 1H, J = 2.3 Hz), 3.32 (q, 4H, J = 7.1 Hz), 1.16 (t, 6H, J = 7.1 Hz). ^{13}C NMR (75 MHz, $CDCl_3$): δ 163.33, 157.96, 155.74, 152.72, 151.29, 136.90, 135.28, 129.90, 125.87, 124.48, 122.27, 121.08, 113.97, 107.93, 107.86, 96.59, 44.68, 12.42. HRMS (ESI$^+$): m/z calcd for $[M + H]^+$ 350.1327, found 350.1314.

Preparation of 4. The same procedure as described for the preparation of **3** was followed, except that 2,3,6,7-tetrahydro-8-hydroxy-1*H*,5*H*-benzo[*ij*]quinolizine-9-carbaldehyde was used (yield 97%). ^{1}H NMR (300 MHz, $CDCl_3$): δ 8.01 (d, 1H, J = 8.1 Hz), 7.89 (d, 1H, J = 7.9 Hz), 7.49−7.44 (m, 1H), 7.36−7.31 (m, 1H), 6.89 (s, 1H), 3.31−3.26 (m, 4H), 2.87 (t, 5.9 Hz), 2.75 (t, 6.2 Hz), 2.02−1.93 (m, 4H). ^{13}C NMR (75 MHz, $CDCl_3$): δ 163.69, 158.39, 152.92, 150.82, 146.76, 137.45, 135.50, 126.36, 125.93, 124.41, 122.27, 121.19, 117.57, 113.30, 107.81, 105.83, 50.09, 49.65, 27.32, 21.43, 20.53, 20.22. HRMS (ESI$^+$): m/z calcd for $[M + H]^+$ 374.1327, found 374.1282.

Preparation of ZnIC. A mixture of **4** (0.30 g, 0.80 mmol), **5** (0.30 g, 1.6 mmol), and acetic acid (0.46 mL, 8 mmol) in 100 mL of dry ethanol was refluxed for 5 h under argon. After evaporation of the ethanol, the residue was diluted with 100 mL of 2 M sodium carbonate and extracted with dichloromethane. The collected organic phase was washed with brine, dried over sodium sulfate, and evaporated to dryness. The residue was chromatographed on silica gel to afford ZnIC (0.39 g, 80%). ^{1}H NMR (300 MHz, $CDCl_3$): δ 8.48−8.46 (m, 2H), 8.38 (s, 1H), 8.01 (m, 1H), 7.88−7.85 (m, 1H), 7.63−7.60 (m, 2H), 7.48−7.40 (m, 3H), 7.34−7.29 (m, 1H), 7.04−6.99 (m, 2H), 6.86 (s, 1H), 3.99 (s, 4H), 3.86 (t, 2H, J = 6.5 Hz), 3.26−3.17 (m, 4H), 3.10 (t, 2H, J = 6.5 Hz), 2.73 (t, 2H, J = 6.2 Hz), 2.65 (t, 2H, J = 6.2 Hz), 1.98−1.88 (m, 4H). ^{13}C NMR (75 MHz, $CDCl_3$): δ 162.97, 160.32, 152.32, 150.54, 148.93, 148.73, 145.95, 137.21, 136.24, 134.48, 126.30, 125.61, 121.22, 117.22, 115.86, 107.91, 106.24, 61.01, 55.49, 50.07, 49.55, 44.26, 29.67, 27.34, 21.59, 20.66, 20.11. HRMS (ESI$^+$): m/z calcd for $[M + H]^+$ 599.2593, found 599.2624.

Acknowledgment. This work was supported in part by the Ministry of Education, Culture, Sports, Science and Technology of Japan (Grants for The Advanced and Innovational Research Program in Life Sciences, 16370071 and 16659003 to T.N. and 14103018, 16651106, 16689002, and 18038008 to Y.U.). T.N. was also supported by the Hoansha Foundation.

JA072432G